OXFORD GENETICS

GENETICS, 2022, 220(3), iyab217
https://doi.org/10.1093/genetics/iyab217
Advance Access Publication Date: 27 November 2021
Investigation

An extracellular matrix damage sensor signals through membrane-associated kinase DRL-1 to mediate cytoprotective responses in *Caenorhabditis elegans*

Keon Wimberly* and Keith P. Choe*

Department of Biology and Genetics Institute, University of Florida, Gainesville, FL 32611, USA

*Corresponding author: Email: kchoe@ufl.edu (K.P.C.); kwimberl1@ufl.edu (K.W.)

Abstract

We and others previously identified circumferential bands of collagen named annular furrows as key components of a damage sensor in the cuticle of *Caenorhabditis elegans* that regulates cytoprotective genes. Mutation or loss of noncollagen secreted proteins OSM-7, OSM-8, and OSM-11 activate the same cytoprotective responses without obvious changes to the cuticle indicating that other extracellular proteins are involved. Here, we used RNAi screening to identify protein kinase DRL-1 as a key modulator of cytoprotective gene expression and stress resistance in furrow and extracellular OSM protein mutants. DRL-1 functions downstream from furrow disruption and is expressed in cells that induce cytoprotective genes. DRL-1 is not required for the expression of cytoprotective genes under basal or oxidative stress conditions consistent with specificity to extracellular signals. DRL-1 was previously shown to regulate longevity *via* a "Dietary Restriction-Like" state, but it functions downstream from furrow disruption by a distinct mechanism. The kinase domain of DRL-1 is related to mammalian MEKK3, and MEKK3 is recruited to a plasma membrane osmosensor complex by a scaffold protein. In *C. elegans*, DRL-1 contains an atypical hydrophobic C-terminus with predicted transmembrane domains and is constitutively expressed at or near the plasma membrane where it could function to receive extracellular damage signals for cells that mount cytoprotective responses.

Keywords: stress response; extracellular matrix; cuticle; receptor; signaling; collagen

Introduction

Cellular and organismal homeostasis are essential for animal development, reproduction, and healthy aging (Cannon 1929; José De Rosa *et al.* 2018). Within cells, cytoprotective gene activation promotes homeostasis during environmental stress, aging, and disease (José De Rosa *et al.* 2018). Subsets of cytoprotective genes tailored to specific conditions are regulated by distinct intracellular sensors and signaling mechanisms (Fontana *et al.* 2010; Fulda *et al.* 2010; Shore *et al.* 2012; Kishimoto *et al.* 2018). For example, metazoan detoxification responses regulated by electrophile-sensitive cap-n-collar transcription factors promote longevity and reduce the occurrence or severity of cancer, chronic inflammation, and neurodegenerative disease (Lewis *et al.* 2010; Tang and Choe 2015; Tebay *et al.* 2015; Lin *et al.* 2018). Mammalian osmotic stress responses regulated by transcription factor NFAT5 are essential for homeostasis of cells in the renal medulla (Beck *et al.* 1998; Danziger and Zeidel 2015) and influence inflammation and extracellular matrix deposition in joints (Sadowska *et al.* 2018).

Epidermal tissues include extracellular matrices that are physical barriers to mechanical insults, pathogens, toxins, and osmotic imbalances (Zhang *et al.* 2015). Although regulation of cytoprotective gene responses *via* intracellular chemical signaling is well-studied, little is known about regulation *via* extracellular mechanical signals. It is becoming increasingly clear that cytoprotective responses can be regulated by structural perturbations in the epidermis. For example, mechanical wounding of epidermal tissues induces antimicrobial peptide expression in humans, *Drosophila*, and *Caenorhabditis elegans* (Sørensen *et al.* 2006; Pujol *et al.* 2008a; Patterson *et al.* 2013; Zhang *et al.* 2015), and disruption of actin polymerization was shown to activate a detoxification response in mouse epidermal cells (van der Kammen *et al.* 2017).

Caenorhabditis elegans is a powerful model for understanding molecular and genetic mechanisms. A defining feature of nematodes is a collagen-rich barrier and exoskeleton termed the cuticle (Cox *et al.* 1981; Page and Johnstone 2007; Chisholm and Hsiao 2012). *Caenorhabditis elegans* cuticle collagens are encoded by over 150 genes and are synthesized and secreted by underlying epidermal cells (Cox *et al.* 1981; Page and Johnstone 2007; Chisholm and Hsiao 2012). Loss or mutation of 21 of these collagens cause obvious morphological and behavior phenotypes (Page and Johnstone 2007). Genome-wide genetic screens for regulators of osmotic and innate immune genes identified some of these cuticle collagens suggesting a link between the cuticle and stress responsive gene regulation (McMahon *et al.* 2003; Wheeler and Thomas 2006; Dodd *et al.* 2018). We and others recently used RNAi to systematically test collagens and other epidermal integrity genes for

Received: August 27, 2021. **Accepted:** November 12, 2021

regulation of six distinct stress responses and discovered that six specific collagens (*dpy-2, 3, 7, 8, 9,* and 10) are required for regulation of osmotic, detoxification, and innate immune responses, but not heat shock or organelle-specific unfolded protein responses (Dodd *et al.* 2018). These six collagens are required for positioning of circumferential bands of collagen termed annular furrows (McMahon *et al.* 2003; Thein *et al.* 2003; Dodd *et al.* 2018). Therefore, furrows are associated with an extracellular sensor for cuticle damage that regulates adaptive stress response genes in underlying cells (Dodd *et al.* 2018).

Other extracellular proteins are also involved in regulating the same three stress responses. Loss of three noncollagen extracellular proteins secreted from epidermal cells (OSM-7, OSM-8, and OSM-11) cause strong constitutive activation of osmotic stress response genes without obvious cuticle phenotypes (Solomon *et al.* 2004; Wheeler and Thomas 2006; Rohlfing *et al.* 2011). Loss of OSM-11 was also shown to activate the detoxification response (Dresen *et al.* 2015). OSM-7 and -11 are secreted or transmembrane proteins that have been linked to extracellular Notch signaling (Komatsu *et al.* 2008; Singh *et al.* 2011). OSM-8 is a mucin-like glycoprotein, which form hydrated gels that function as lubricants and signaling modifiers (Rohlfing *et al.* 2011). Prior epistasis analysis demonstrates that osmolyte accumulation is nonadditive when *osm-7* loss is combined with furrow disrupting alleles of *dpy-2*, *dpy-7*, or *dpy-10* consistent with functional overlap (Wheeler and Thomas 2006).

These studies establish a specific collagen structure and other extracellular proteins as regulators of conserved stress responses, but downstream signaling is largely unknown. Here, we used RNAi to screen protein kinases for regulation of stress response genes in a furrow collagen mutant. Loss of *drl-1*, Dietary Restriction-Like kinase, caused the most consistent suppression of stress response gene expression. DRL-1 has an N-terminal kinase domain homologous to mammalian MEKK-3, which has been implicated in regulating cell osmotic responses *via* p38 MAPK (Uhlik *et al.* 2003; Padda *et al.* 2006; Craig *et al.* 2008). Loss of *C. elegans drl-1* was previously shown to increase fat metabolism and extend lifespan by a mechanism similar to dietary restriction (Chamoli *et al.* 2014). We find that DRL-1 is required for full activation of detoxification, osmotic, and innate immune responses in worms with mutations in annular furrow collagens or extracellular proteins OSM-7 or OSM-8. Loss of *drl-1* does not reduce expression of the same stress response genes under basal or oxidative stress conditions consistent with specificity. Genetic interaction analyses suggest that DRL-1 mediates cytoprotective gene expression by a mechanism that is independent of dietary restriction and the p38 MAPK pathway. Loss of *drl-1* from either the epidermis or intestine partially suppresses cytoprotective gene expression in a furrow collagen mutant consistent with cell autonomous regulation. DRL-1 protein is predicted to contain three C-terminal transmembrane domains, and DRL-1::GFP colocalizes with a plasma membrane specific dye. Therefore, DRL-1 is positioned where it could function at the surface of cells to receive and transduce extracellular damage signals originating from the cuticle.

Materials and methods

Caenorhabditis elegans strains

All strains were cultured and maintained at 20°C under standard conditions unless mentioned otherwise (Brenner 1974). The following strains were used: wild-type N2 Bristol, CB128 *dpy-10(e128)*, CB88 *dpy-7(e88)*, QV248 *dpy-7(e88); dvIs19[gst-4p::GFP]*, QV261 *dpy-7(e88); kbIs24[gpdh-1p::DsRed2; myo-2p::GFP; unc-119 rescue]*, IG1689 *dpy-7(e88); frIs7[nlp-29p::GFP + col-12p::GFP]*, QV337 *drl-1(vir11)*, QV341 *dpy-10(e128); drl-1(vir11)*, QV342 *dpy-7(e88); drl-1(vir11)*, TP12 *kaIs12*[COL-19::GFP], QV329 *dpy-10(e128); kaIs12*, HA1857 *osm-7(tm2256)*, MT3571 *osm-8(n1518)*, QV346 *dpy-10(e128); eat-2(ad465)*, QV334 *dpy-10(e128); nhr-49(nr2041)*, QV356 *dpy-10(e128); rde-1(ne219)*, QV348 *dpy-10(e1289); rde-1(ne219), kzIs9 [(pKK1260) lin-26p::NLS::GFP, (pKK1253) lin-26p::rde-1; rol-6(su1006)]*, QV343 *dpy-10(e128); rde-1(ne219); kbIs7 [nhx-2p::rde-1 + rol-6(su1006)]*, QV355 *zjEx144 [drl-1::GFP; myo-2p::tdTomato]*, QV361 *zjEx145[drl-1p::GFP; myo-2p::tdTomato]*, QV362 *zjEx146[drl-1p including intron 1::GFP; myo-2p::tdTomato]*.

RNAi experiments

An RNAi screen targeting 381 protein kinase genes was performed by feeding worms with *Escherichia coli* [HT115(DE3)] engineered to synthesize double-stranded RNA (dsRNA). RNAi clones were taken from the ORFeome RNAi feeding library (Open Biosystems, Huntsville, AL) and missing clones were supplemented from the MRC genomic library (Geneservice, Cambridge, UK). Synchronized QV248, QV261, and IG1689 L1 larvae were grown on liquid or agar nematode growth medium (NGM) supplemented with 25 μg/ml carbenicillin and 3 mM isopropyl β-d-1-thiogalactopyranoside (IPTG). All worm strains were fed dsRNA-producing bacteria for 2–3 days and screened manually for suppression of fluorescence with a Zeiss Stemi SV12 microscope. Phenotypes were scored as follows: 0, no suppression in >50% of worms; 0.5, suppression in >50% of worms but also sickness; 1, partial suppression in >50% of worms without sickness; and 2, full suppression in >50% of worms without sickness.

For subsequent RNAi experiments, worms were grown on agarose NGM plates supplemented with 25 μg/ml carbenicillin and 3 mM isopropyl β-d-1-thiogalactopyranoside (IPTG). Synchronized L1s were fed dsRNA bacteria for 2–3 days and allowed to develop to L4 larvae or young adults before being used for experiments. The control RNAi clone was pPD129.36 (LH4440); it encodes a 202-bp dsRNA that is not homologous to any *C. elegans* gene.

Transgenic reporter generation and microscopy

GFP constructs were generated with PCR fusion as we have described previously (Hobert 2002; Choe *et al.* 2009; Wu *et al.* 2017). For one transcriptional construct, a ~2.5 kb region upstream of the *drl-1* start codon was fused with GFP; for the longer transcriptional construct, the same ~2.5 kb upstream region, exon 1, and the first intron of the *drl-1* locus were fused with GFP at the start of exon 2; for the translational construct, the ~2.5 kb region upstream of the *drl-1* start codon along with the rest of the *drl-1* locus (excluding intron 1) was fused to GFP just before the stop codon; intron one is large (2609 bp) and was excluded to facilitate amplification.

Worms were mounted on 2% agarose pads with 5 mM levamisole and imaged using an Olympus BX60 microscope with a Zeiss AxioCam MRm camera fitted with either a GFP or RFP filters. Exposure settings were consistent for each strain. Color was added using ImageJ Version 1.53c; adjustments to contrast and brightness were made evenly to whole images. Dissected intestines were stained with 1.5 ug/mL CellMask Orange plasma membrane stain (Life Technologies, Cat No. C10045) for 10 min in NGM buffer and fixed in 2% formaldehyde for 10 min before imaging on 0.5% agarose pads. Colocalization was quantified in the intestine with Image J plugin "JaCoP."

Quantitative PCR

Worms were washed and lysed *via* sonication and RNA was purified using Zymo Research RNA MicroPrep kit (Cat. no. R1051). Each of these samples were then treated with dsDNAse from ThermoFisher (Cat. no. EN0771). cDNA was synthesized using Promega GoScript Reverse Transcriptase (REF A5004) with oligo(dT)15 primers. Quantitative PCR (qPCR) assays were performed in an Eppendorf RealPlex2 using primers for *rpl-2* and *cdc-42* as reference genes. Primer sequences are available upon request.

High salt motility assay

Young adult worms were transferred (*via* chunking) to agar plates supplemented with high salt levels and without bacteria. Chunks were slid and removed leaving worms on the surface of high salt agar. After 10 min, the total and number of worms able to make lateral movement were counted. At least 20 total worms were scored for each replicate.

Glycerol assay

Synchronized adults were lysed *via* sonication as performed previously with a BioVision PicoProbe Free Glycerol Assay Kit (K643-100) (Dodd *et al.* 2018). Glycerol concentrations were normalized to total protein content in each sample using a Thermo Scientific Pierce BCA Protein Assay Kit (23225).

Statistical analysis

Statistical significance was determined using a Student's *t*-test when two means were compared. *P*-values of < 0.05 were taken to indicate statistical significance. For experiments with multiple gene comparisons, the Benjamini-Hochberg method was used to determine which *P*-values remained significant at an FDR of 5%. All graphs were generated using PRISM 5.04 software (La Jolla, CA, USA).

Results

drl-1 is required for cytoprotective gene activation in cuticle furrow mutants

To identify regulators of cytoprotective responses downstream from furrow disruption, we generated *dpy-7(e88)* annular furrow mutant strains carrying fluorescent transcriptional reporters for core organic osmolyte (*gpdh-1*), detoxification (*gst-4*), and innate immune (*nlp-29*) stress response genes (Figure 1A). These strains were used in RNAi screens of 381 predicted protein kinases and average scores for clones with reproducible effects are summarized as a heat map in Figure 1B. Clone *drl-1* caused the most consistent suppression of *gpdh-1*, *gst-4*, and *nlp-29* reporters (Figures 1B and 2A). Suppression by *drl-1* RNAi was confirmed using qRT-PCR in *dpy-7(e88)* and *dpy-10(128)* annular furrow mutants (Figure 2B). In addition to the genes tested in the initial screens, *drl-1* RNAi suppressed additional core osmolyte accumulation (*hmit-1.1*) and detoxification (*gst-10*) genes in *dpy-7* and *dpy-10* worms (Figure 2B).

In wild-type worms under basal conditions, *drl-1* RNAi did not decrease expression of osmolyte accumulation genes, *gst-4*, or *nlp-29* (Figure 2B). Alternatively, *drl-1* RNAi suppressed *gst-10* expression by at least 80% in wild-type and *dpy* worms. These results suggest that *drl-1* is dispensable for osmolyte accumulation and *nlp-29* gene expression under basal conditions but may have a broader role in regulating some detoxification genes.

The original *drl-1* dsRNA clone targets exons 2-10; *drl-1* mRNA levels are reduced over 80% by this clone confirming silencing (Figure S1A and B). To evaluate specificity, we generated and tested two nonoverlapping dsRNA clones targeting *drl-1* as previously reported (Chamoli *et al.* 2014). One of these new *drl-1* dsRNA clones targets exons 2-5 and part of 6; the second one targets the rest of exon 6, and exons 7-10 (Figure S1A). Both nonoverlapping *drl-1* dsRNA clones suppressed all three stress-response reporters in *dpy-7* worms similar to the original clone (Figure S1C).

Cytoprotective gene expression was also analyzed with a *drl-1(vir11)* allele crossed with *dpy-7(e88)* and *dpy-10(e128)*. A *drl-1* null allele is not available and would be expected to cause embryonic lethality and sterility based on RNAi phenotypes (Kamath *et al.* 2003). The *drl-1(vir11)* allele was isolated from a mutagenesis screen for altered viral responses (Sandoval *et al.* 2019); it contains a G-to-A mutation at the splice acceptor site for the ninth exon and a G-to-A missense mutation resulting in a D522N amino acid substitution (Figure S1A). Functional consequences of D522N are difficult to predict because it is located well outside of the putative kinase domain. Total *drl-1* mRNA levels are slightly increased in *drl-1(vir11)* worms (Figure S1D); we detected altered splicing of exons 8 and 9 in a fraction of transcripts amplified with RT-PCR and visualized by gel electrophoresis (Figure S1E). Intron 8 is a multiple of 3 (42), and its retention is not predicted to change reading frame or introduce a stop codon. Real-time PCR demonstrated that *drl-1(vir11)* suppresses osmotic, detoxification, and innate immune response genes in *dpy-7* and *dpy-10* worms similar to *drl-1* RNAi except for *gpdh-1* (Figure S1F) providing further evidence that *drl-1* influences cytoprotective gene expression. However, given uncertainty about the exact functional consequence of *vir11* on DRL-1 function, we use *drl-1* RNAi for the remainder of functional experiments.

Loss of *drl-1* reduces glycerol and osmotic stress resistance in annular furrow mutants

C. elegans accumulates the osmolyte glycerol when exposed to hypertonic stress (Lamitina and Strange 2005; Choe and Strange 2007a, 2007b; Choe 2013). Organic osmolyte accumulation helps balance high environmental osmolarity and can limit acute hyperosmotic water loss (Lamitina and Strange 2005; Choe and Strange 2007b; Choe 2013). Furrow mutants have elevated glycerol levels compared to wild type worms under standard culture conditions (Lamitina *et al.* 2006; Wheeler and Thomas 2006; Dodd *et al.* 2018). As shown in Figure 2, A and B, *drl-1* loss suppresses *gpdh-1* in furrow mutants; *gpdh-1* encodes a rate-limiting enzyme for glycerol synthesis (Lamitina and Strange 2005; Lamitina *et al.* 2006). As shown in Figure 2C, *drl-1* RNAi reduced glycerol accumulation in *dpy-7(e88)* and *dpy-10(e128)* worms by 60% and 35%, respectively.

Hypertonic water loss causes collapse of the nematode hydrostatic skeleton and paralysis within minutes (Lamitina and Strange 2005; Wheeler and Thomas 2006; Choe and Strange 2007a, 2007b; Burkewitz *et al.* 2012; Choe 2013); annular furrow mutants have an acute "OSmotic Resistant" (OSR) phenotype that allows them to remain mobile (Wheeler and Thomas 2006). To test if *drl-1* loss suppresses OSR, we ran motility assays with and without *drl-1* RNAi in *dpy-7* and *dpy-10* mutants. Worms were grown under standard conditions (51 mM NaCl) and transferred to high salt (800 mM or 700 mM NaCl) plates as young adults; these salt levels were selected for roughly 80–90% motility in each *dpy* strain (Figure 2D). After 10 min, the number of motile and paralyzed worms was counted on each plate; as expected, all

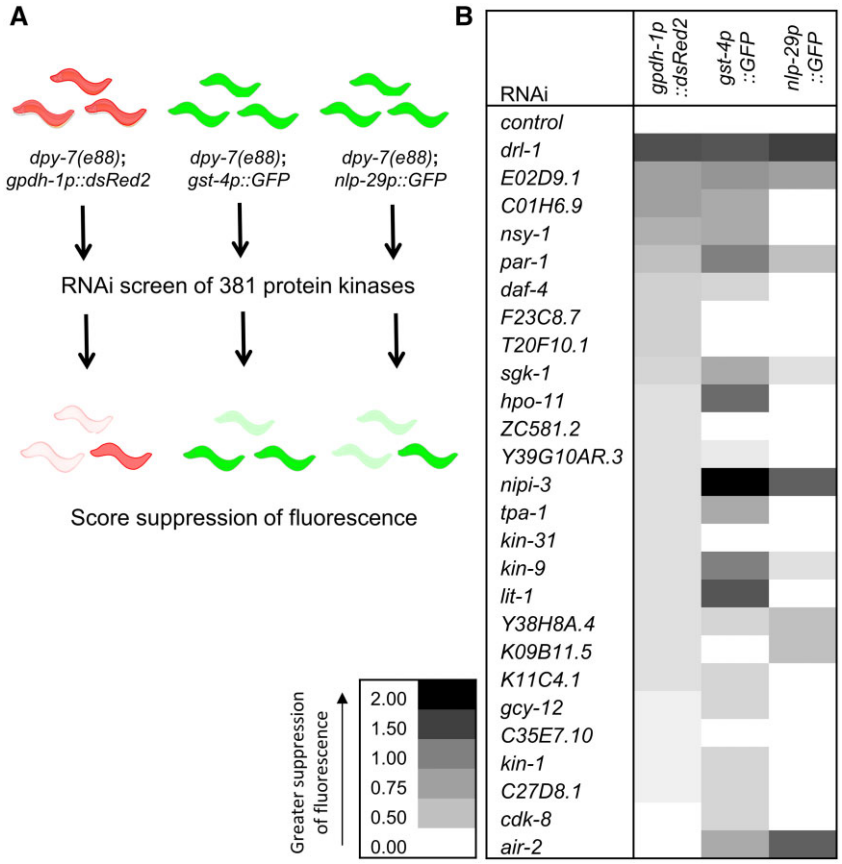

Figure 1 Protein kinase screen for suppressors of stress responses in an annular furrow mutant. (A) Schematic of three parallel RNAi screens to identify protein kinases required for activation of organic osmolyte (*gpdh-1*), detoxification (*gst-4*), and innate immune (*nlp-29*) genes in *dpy-7(e88)* worms. (B) Heat map of average fluorescence suppression scores for dsRNA clones that reproducibly suppressed at least one of the three reporters. The heat map reflects average scores for six (*gpdh-1* reporter) or four (*gst-4* and *nlp-29* reporters) trials. For each trial, 30–40 worms were fed dsRNA from the L1 to young adult stage and scored based on fluorescence. Entire populations of worms were scored manually as follows: 0, no suppression in >50% of worms; 0.5, suppression in ≥50% of worms but also some sickness; 1, partial suppression in ≥50% of worms without sickness; and 2, full suppression in ≥50% of worms without sickness.

wild type worms were paralyzed and over 80% of *dpy-7* and *dpy-10* worms with control RNAi were motile after 10 min. Motility was reduced to below 40% when *dpy-7* and *dpy-10* worms were grown on *drl-1* dsRNA before transfer to hypertonicity (Figure 2D). Taken together, the results in Figure 2 demonstrate that *drl-1* is required in furrow mutants for full activation of cytoprotective genes and biochemical and physiological osmotic responses.

DRL-1 does not influence furrow organization and functions beyond larval development

Cuticle furrow organization is one possible mechanism by which *drl-1* could be required for stress responses in *dpy-7* and *dpy-10* mutants. Organization of furrows can be visualized in adult worms using COL-19::GFP, a collagen reporter that permits visualization of furrows (Thein *et al.* 2003; Dodd *et al.* 2018). No obvious change in furrow organization was observed with *drl-1* RNAi in wild type worms (Figure 3). Furthermore, *drl-1* RNAi did not suppress furrow disorganization in *dpy-7* or *dpy-10* worms (Figure 3) consistent with DRL-1 functioning downstream from the cuticle.

Although *drl-1* loss did not affect furrow organization, it was still possible that *drl-1* could be required for another larval development process that is important to cuticle damage signaling. Figure S2A shows stress response gene expression in adult *dpy-7* worms with *drl-1* dsRNA feeding started at L1 or L4; the L4 group was fed control dsRNA until L4. The effects of *drl-1* RNAi were similar or stronger in the L4 group than L1 group for *gpdh-1*, *hmit-1.1*, and *gst-4* (Figure S2A); *drl-1* RNAi effects in the L4 group were weaker but still significant for *gst-10* and not-significant for *nlp-29*. These data demonstrate that DRL-1 is required for osmotic and detoxification gene expression in a furrow mutant beyond the time when most larval development is complete.

Loss of *drl-1* suppresses stress responses in osm-7 and osm-8 mutants

Given that loss of extracellular OSM proteins activates the same stress responses as furrow loss (Wheeler and Thomas 2006; Rohlfing *et al.* 2011; Dresen *et al.* 2015; Dodd *et al.* 2018) and that the two mutant classes functionally interact (Wheeler and Thomas 2006), we also tested the role of *drl-1* in *osm-7* and *osm-8* mutants. As shown in Figure 4, A–D, *osm-7* and *osm-8* loss-of-function mutations induce stress response genes, glycerol accumulation, and OSR similar to furrow disruption. Loss of *drl-1* suppresses all of these phenotypes (Figure 4, A–D). These results suggest that DRL-1 is a common regulator of cytoprotective gene responses downstream from furrow collagens and noncollagen extracellular OSM proteins.

Results for *drl-1* in furrow collagen and OSM mutants (Figures 2 and 4) raised the possibility of broad involvement in

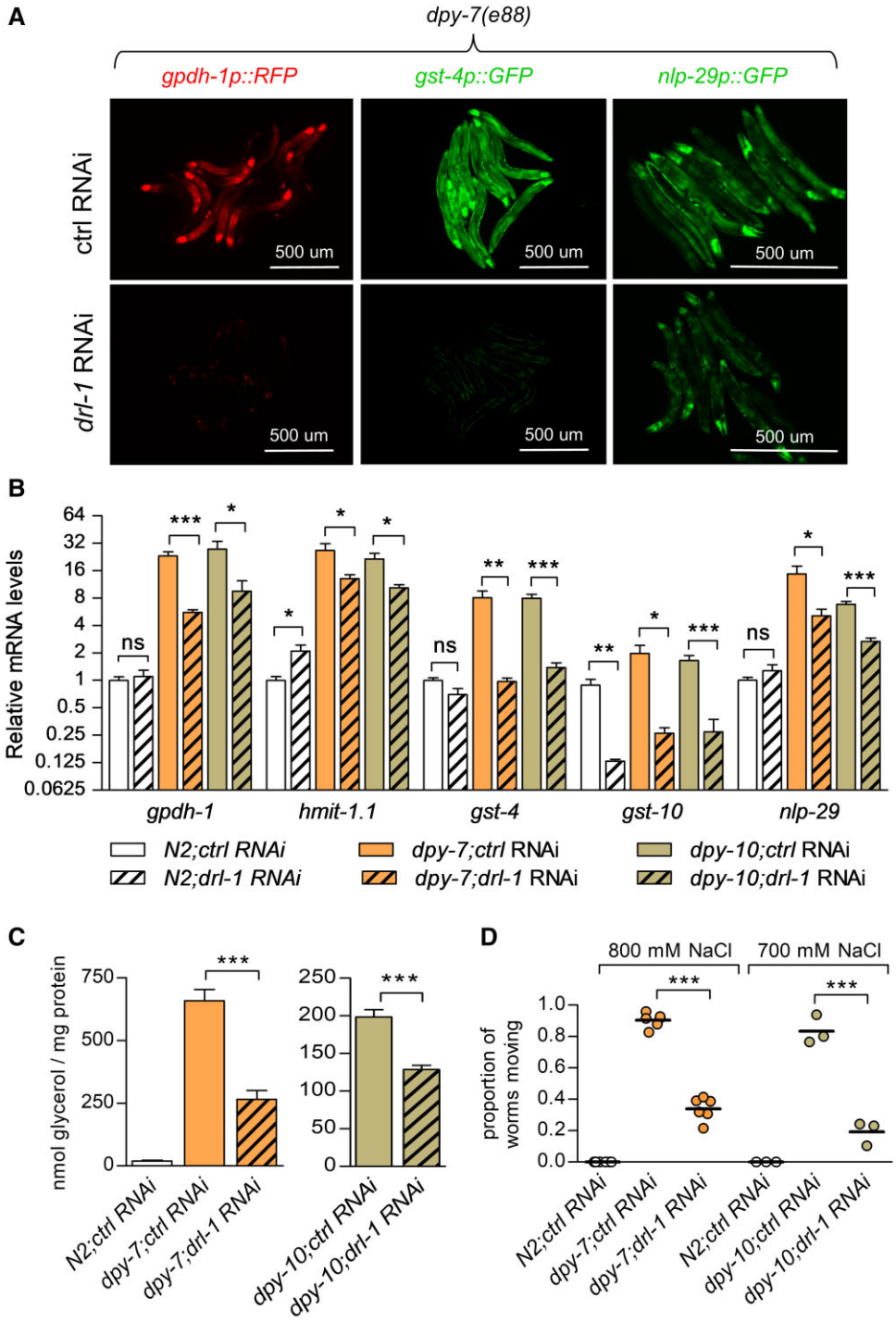

Figure 2 *drl-1* is required for stress response activation in furrow collagen mutants. (A) *dpy-7(e88)* furrow mutants carrying an osmotic (*gpdh-1*), detoxification (*gst-4*), or innate immunity (*nlp-29*) fluorescent transgene; worms were fed control or *drl-1* dsRNA. (B) mRNA levels for cytoprotective genes in *dpy-7(e88)* and *dpy-10(e128)* furrow mutants fed control or *drl-1* dsRNA. Values are normalized to N2 worms fed control dsRNA. $N = 5$ to 9 populations of worms from 2 to 3 trials. (C) Whole-worm glycerol levels in N2, *dpy-7(e88)*, and *dpy-10(e128)* worms treated with control or *drl-1* dsRNA. $N = 5$–23 populations of worms from 2 to 6 trials. (D) Worm motility 10 min after transfer to agar containing indicated levels of NaCl. $N = 3$–6 populations of worms from 1 to 2 trials. (B-D) $^{***}P < 0.001$, $^{**}P < 0.01$, and $^{*}P < 0.05$.

adaptive responses to cuticle disruption. Therefore, we next tested a distinct class of cuticle mutant. BLI-4 is a protease in the subtilisin-convertase family (Thacker *et al.* 1995); loss of *bli-4* causes molting defects and strong activation of an *nlp-29* transcriptional reporter without activation of *gpdh-1* or *gst-4* (Dodd *et al.* 2018). As shown in Figure S2B, *bli-1(e937)* strongly activated *nlp-29* to the same degree with or without *drl-1* RNAi indicating that *drl-1* is not required for response to this molting defect.

drl-1 regulation of cytoprotective responses is condition-dependent

Hypertonicity induces osmolyte, detoxification, and innate immune response genes similar to furrow disruption raising the

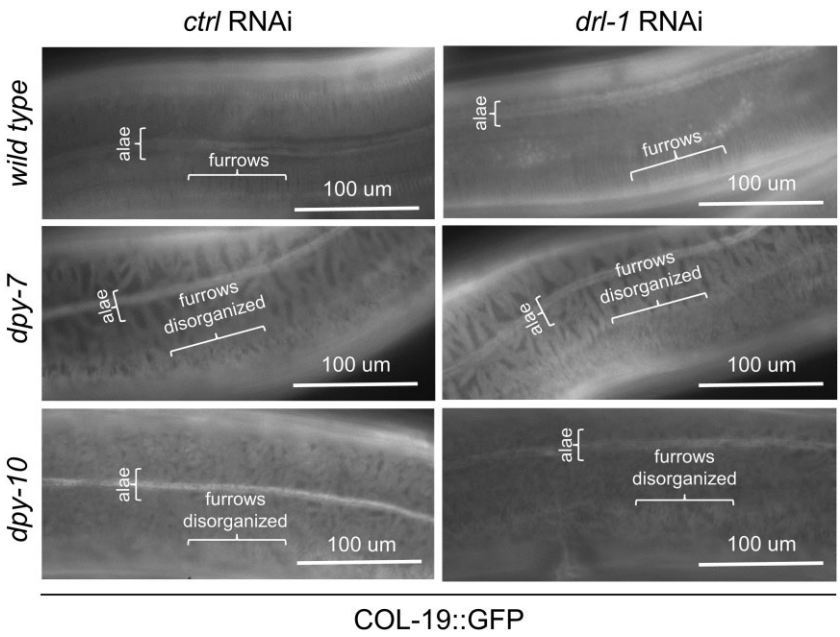

Figure 3 Loss of *drl-1* has no obvious effect on furrow organization. Fluorescence micrographs of N2, *dpy-7(e88)*, and *dpy-10(e128)* worms expressing *col-19::GFP* and fed control or *drl-1* dsRNA.

possibility that furrow disorganization mimics physical distortion that occurs during hypertonicity (Lamitina and Strange 2005; Lamitina *et al.* 2006; Wheeler and Thomas 2006; Pujol *et al.* 2008b; Choe 2013; Dodd *et al.* 2018). To determine if DRL-1 is also required for cytoprotective responses in wild-type worms during hypertonicity, we performed qRT-PCR in control and *drl-1* RNAi-treated wild-type worms grown on 200 mM NaCl (Lamitina *et al.* 2004; Rohlfing *et al.* 2010). Similar to results in *dpy-7* and *dpy-10* worms (Figure 2B), *drl-1* RNAi strongly suppressed *gst-4* and *gst-10* over fivefold in worms grown on 200 mM NaCl (Figure 5A). Alternatively, *drl-1* RNAi only suppressed *gpdh-1* and *nlp-29* by 1.8- and 1.5-fold, respectively in worms grown at 200 mM NaCl (Figure 5A) compared to over 4.0- and 2.9-fold in *dpy-7* worms (Figure 2B). *drl-1* RNAi had no effect on *hmit-1.1* in worms grown at 200 mM NaCl (Figure 5A).

Exposure to 200 mM NaCl increases glycerol accumulation and OSR (Lamitina *et al.* 2004). Consistent with a small effect on osmolyte accumulation genes (Figure 5A), *drl-1* RNAi did not suppress glycerol accumulation or OSR in worms grown at 200 mM NaCl (Figure 5, B and C). Taken together, these results suggest that other parallel mechanisms largely compensate for loss of *drl-1* during osmotic stress to activate *gpdh-1*, *hmit-1.1*, and *nlp-29*, but not *gst-4*. Surprisingly, *drl-1* RNAi increased glycerol levels in wild-type worms under basal conditions (Figure 5B) without affecting *gpdh-1* expression (Figure 2B). Previously reported changes to fatty acid metabolism by *drl-1* RNAi could yield free glycerol independent of *gpdh-1* (Arner 2005; Chamoli *et al.* 2014). Regardless of the mechanism, *drl-1* RNAi did not increase OSR in wild-type worms (Figure 5C).

In contrast to osmotic (*gpdh-1 and hmit-1.1*) and innate immune response genes (*nlp-29*), *drl-1* RNAi strongly suppressed *gst-4* expression in worms exposed to 200 mM NaCl (Figure 5A) and suppressed *gst-10* under all conditions tested suggesting a broader role for detoxification genes. We explored the role of DRL-1 in detoxification gene expression further by measuring five detoxification genes under basal and oxidative stress conditions using qRT-PCR. Under basal conditions, *drl-1* RNAi significantly suppressed transcription of two of the five detoxification genes analyzed, *gst-10* and 30 (Figure S4). Arsenite and acrylamide are electrophile and pro-oxidant molecules that strongly activate SKN-1 dependent detoxification genes (Hasegawa *et al.* 2008; Oliveira *et al.* 2009; Przybysz *et al.* 2009; Wu *et al.* 2016). As shown in Figure S4, *drl-1* RNAi did not significantly decrease *gst-4, gst-12, gst-30*, or *gcs-1* expression in wild-type worms exposed to 5 mM arsenite or 7 mM acrylamide; *gst-10* was suppressed roughly equally under all conditions. Therefore, *drl-1* is not required for detoxification gene induction by pro-oxidants or electrophiles.

DRL-1 regulates stress responses independently of *nhr-49* and dietary restriction

A previous study reported that loss of *drl-1* in *C. elegans* induces a dietary restriction-like state with increased longevity and oxidation of fat (Chamoli *et al.* 2014). Mutations in pharynx-specific channel EAT-2 reduce feeding and increase life span (Lakowski and Hekimi 1998; Chamoli *et al.* 2014). RNAi of *drl-1* and an *eat-2* mutation were each shown to increase longevity to similar degrees with no additive effect when combined (Chamoli *et al.* 2014). If loss of *drl-1* controls cytoprotective gene expression by the same mechanism, then dietary restriction should also suppress stress responses in furrow mutants. A long-lived *eat-2* allele (Lakowski and Hekimi 1998; Chamoli *et al.* 2014) decreased *gpdh-1* and increased *gst-4* expression in an otherwise wild-type background (Figure S3A). As shown in Figure 6A, *eat-2* mutation (Lakowski and Hekimi 1998; Chamoli *et al.* 2014) suppressed detoxification genes *gst-4* and *gst-10* in *dpy-10* worms, but had no effect on *gpdh-1, hmit-1.1*, or *nlp-29;* effects of *drl-1* RNAi on *gpdh-1*, *hmit-1.1*, and *gst-4* were independent of *eat-2* (Figure 6A).

The dietary restriction like state induced by *drl-1* loss includes an increase in fatty acid beta oxidization (Chamoli *et al.* 2014). When *drl-1* is silenced, beta oxidation genes are regulated by a mechanism that requires nuclear hormone receptor NHR-49 (Van Gilst *et al.* 2005; Pathare *et al.* 2012; Chamoli *et al.* 2014). If the same mechanism functions in furrow mutants, then *nhr-49*

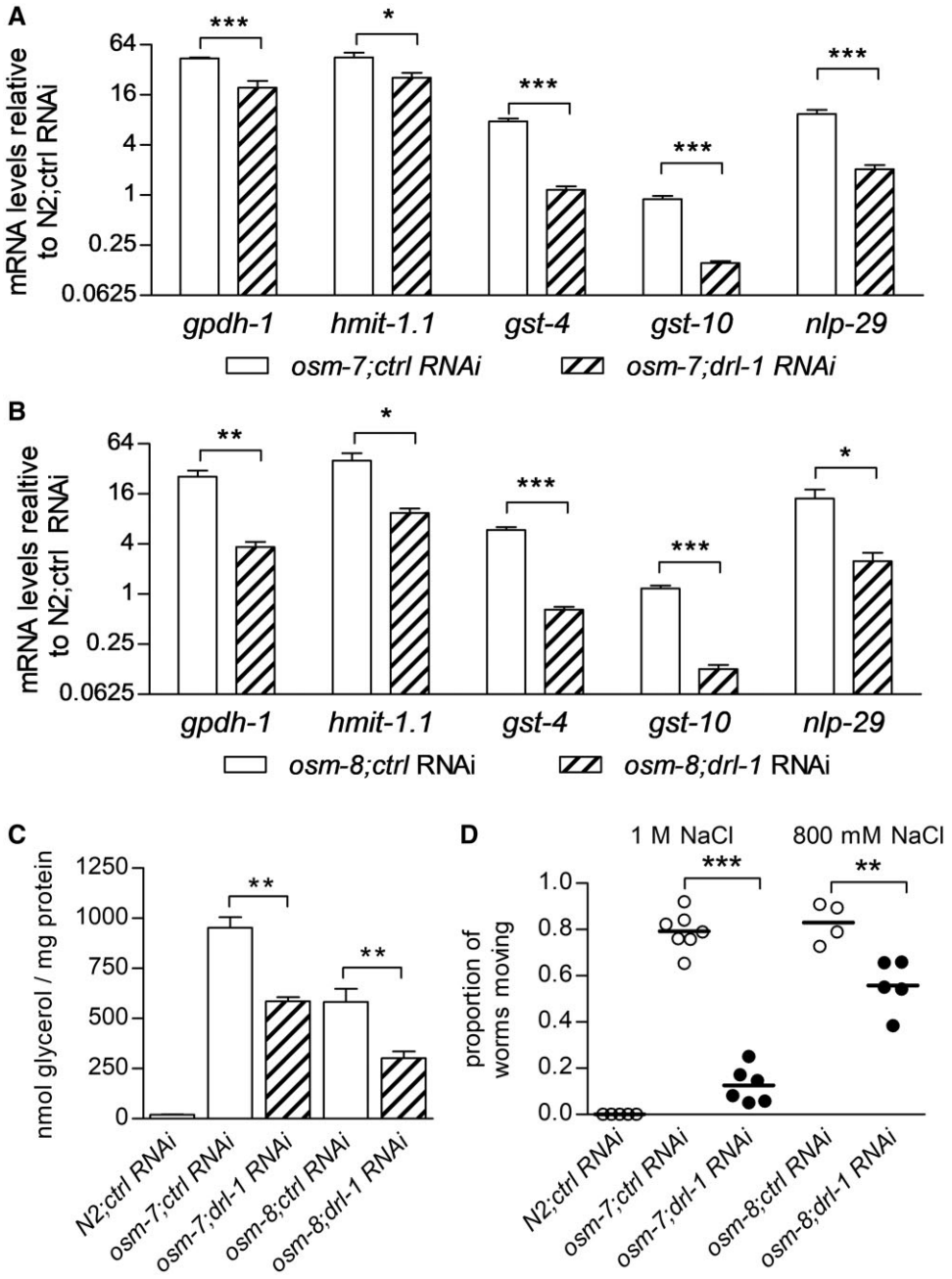

Figure 4 Loss of *drl-1* suppresses stress responses in OSM-7 and OSM-8 mutants. (A, B) mRNA levels of cytoprotective genes in *osm-7(tm2256)* and *osm-8(n1518)* worms fed control or *drl-1* dsRNA. $N = 6$–8 populations of worms from 2 to 3 trials. (C) Whole-worm glycerol levels in N2, *osm-7(tm2256)*, and *osm-8(n1518)* worms fed control or *drl-1* dsRNA. $N = 3$–23 populations of worms from 1 to 6 trials; the same control RNAi, 51 mM NaCl samples are plotted in Figure 2C. (D) Worm motility 10 min after transfer to agar containing indicated levels of NaCl. $N = 4$ to 7 populations from 2 to 3 trials. (A–D) $^{***}P < 0.001$, $^{**}P < 0.01$, and $^{*}P < 0.05$.

should be required for *drl-1* RNAi to suppress cytoprotective genes. In an otherwise wild type background, an *nhr-49(nr2041)* loss-of-function allele decreased *gpdh-1*, *hmit-1.1*, and *gst-4* expression (Figure S3B). In *dpy-10* worms, *nhr-49(nr2041)* increased and decreased *gpdh-1* and *gst-4* expression, respectively (Figure 6B). However, *drl-1* RNAi suppressed cytoprotective genes in *dpy-10* worms independent of *nhr-49* (Figure 6B).

DRL-1 regulates osmolyte and detoxification responses independently of p38 MAPK

Caenorhabditis elegans DRL-1 contains a serine threonine kinase domain homologous to human mitogen-activated protein kinase kinase kinase (MAPKKK) MEKK3 (Chamoli *et al.* 2014; Sandoval *et al.* 2019). MEKK3 was reported to regulate osmotic stress responses *via* p38 MAPK (Uhlik *et al.* 2003; Padda *et al.* 2006). p38 MAPKs regulate responses to stress and inflammatory cytokines in mammalian cells and *C. elegans* (Chang and Karin 2001; Johnson and Lapadat 2002; Kim *et al.* 2002; Tanaka-Hino *et al.* 2002; Chuang and Bargmann 2005; Inoue *et al.* 2005). In *C. elegans*, SKN-1 is regulated directly by p38 MAPK during oxidative stress (Inoue *et al.* 2005) and *nlp-29* is regulated by p38 MAPK following wounding and infection (Ziegler *et al.* 2009).

To determine if DRL-1 regulates cytoprotective responses *via* the p38 pathway in furrow mutants, a *sek-1(km4)* deletion allele

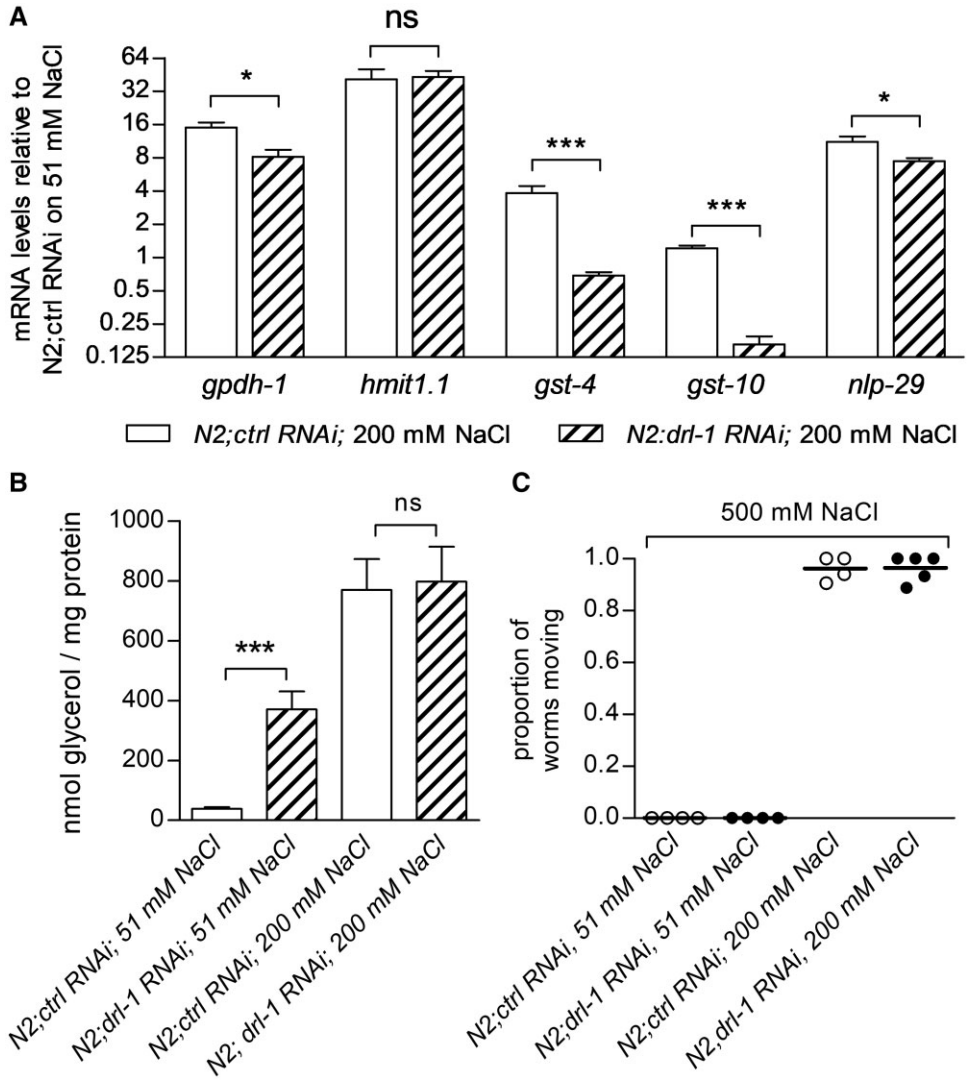

Figure 5 Other mechanisms partially compensate for *drl-1* loss during osmotic stress. (A) mRNA levels of stress response genes in N2 worms fed control or *drl-1* dsRNA and exposed to 200 mM NaCl for 12 h. $N = 5$–6 populations of worms from 2 trials. (B) Whole-worm glycerol levels in N2 worms fed control or *drl-1* dsRNA on standard (51 mM NaCl) or high (200 mM NaCl) levels of salt. $N = 9$–23 populations of worms from 3 to 6 trials. (C) Worm motility 10 min following transfer to 500 mM NaCl. $N = 4$ populations of worms from 1 trial. (A–C) $^{***}P < 0.001$, $^{**}P < 0.01$, and $^{*}P < 0.05$.

was crossed into a *dpy-10* background; *sek-1* encodes p38 MAPKK and is required for p38 MAPK activity (Tanaka-Hino *et al.* 2002). We used *dpy-10* because *dpy-7* is on the same chromosome near *sek-1*. If DRL-1 functions by regulating p38 MAPK, then loss of *sek-1* should suppress cytoprotective genes on its own but not when combined with loss of *drl-1*. Loss of *sek-1* suppressed *gst-4* in *dpy-10* worms on its own, and this effect was independent of *drl-1* RNAi (Figure S5). Loss of *sek-1* suppressed *nlp-29* in *dpy-10* worms but had a smaller, nonsignificant, effect when *drl-1* was silenced (Figure S5). These results are consistent with DRL-1 influencing cytoprotective gene expression by a mechanism that is largely distinct from the p38 MAPK pathway.

DRL-1 is localized at or near plasma membranes

drl-1 mRNA was previously shown to be highly enriched in the epidermis and intestine of *C. elegans* (Pauli *et al.* 2006; Spencer *et al.* 2011; Blazie *et al.* 2017; Han *et al.* 2017), which are the two tissues that highly express osmolyte, detoxification, and antimicrobial response genes (Lamitina *et al.* 2006; Pujol *et al.* 2008a; Lee *et al.* 2010; Kage-Nakadai *et al.* 2011; Choe 2013; Zugasti *et al.* 2016; Dodd *et al.* 2018). Epidermal cells also secrete cuticle collagens and are adjacent to the cuticle (Chisholm and Xu 2012). To gain more insight into tissue distribution, we first fused ~2.5 kb of intergenic sequence upstream from the start codon to GFP coding sequence; this intergenic reporter only drove GFP expression in the intestine (Figure S7). However, *drl-1* contains a large, ~2.6 kb first intron that could include additional regulatory sequences. We generated a more complete *drl-1p*::GFP reporter by fusing GFP coding sequence to a ~5.1 kb genomic fragment that includes the upstream intergenic region and intron 1 and co-injected it with pharynx marker *myo-2p*::tdTomato. As shown in Figure 7A, *drl-1p*::GFP was expressed in the epidermis (*i.e.*, "hyp" cells) and intestine ("int") consistent with previous mRNA enrichment studies (Pauli *et al.* 2006; Spencer *et al.* 2011; Blazie *et al.* 2017; Han *et al.* 2017). These results suggest that the upstream intergenic region drives expression in the intestine and that intron 1 also permits expression in the epidermis. A prior study failed to observe intestinal expression with a *drl-1* transcriptional reporter (Chamoli *et al.* 2014); however, this former construct lacked the intergenic region upstream from exon 1 that drives intestinal expression (Figure S7).

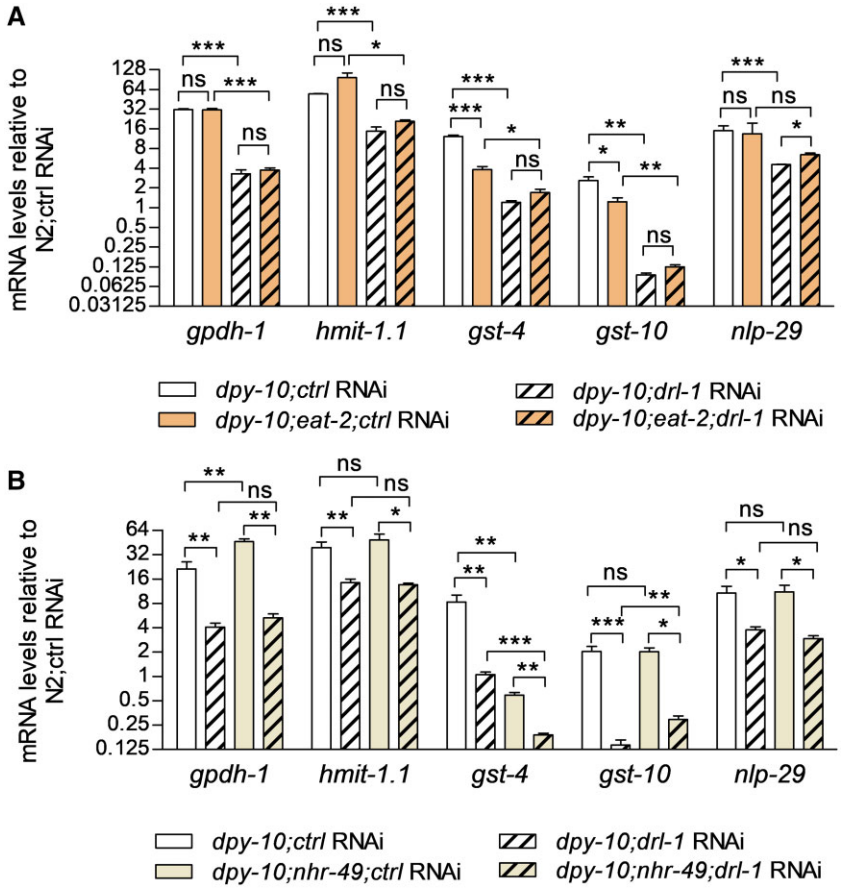

Figure 6 *drl-1* mediates stress responses in furrow mutants independent of a dietary restriction like mechanism. (A) mRNA levels for cytoprotective genes in *dpy-10(e128)* and *dpy-10(e128); eat-2(ad465)* worms fed control or *drl-1* dsRNA. $N = 3$–4 populations of worms from 1 trial. (B) mRNA levels for cytoprotective genes in *dpy-10(e128)* and *dpy-10(e128); nhr-49(nr2041)* worms fed control or *drl-1* dsRNA. $N = 5$–6 populations of worms from 2 trials, $^{***}P < 0.001$, $^{**}P < 0.01$, and $^{*}P < 0.05$.

To gain insights on DRL-1 protein localization, a DRL-1::GFP construct was generated and expressed in wild-type worms; to permit cloning of this large ~8.6 kb construct, we omitted intron 1 and focused on intestine cells, which are large and well-suited for visualizing intracellular localization; as expected, DRL-1::GFP fluorescence was only observed in the intestine. Within the intestine, fluorescence was enriched near the boundaries of cells (Figure 7B). To determine if DRL-1::GFP is at the membrane, we colocalized with amphipathic plasma membrane dye CellMask in dissected and fixed intestines (Wang *et al.* 2013). As shown in Figure 7C, DRL-1::GFP and CellMask colocalize (Pearson's correlation coefficient of 0.69) at cell borders consistent with DRL-1 localization at or near plasma membranes.

DRL-1 is required in the epidermis and intestine for cytoprotective gene transcription in furrow mutants

We next used previously established tissue-specific *rde-1* rescue strains to test if cytoprotective gene expression requires *drl-1* in the epidermis or intestine (Qadota *et al.* 2007). We crossed *rde-1(ne219)* and wildtype *rde-1* rescue constructs with *dpy-10(e128)* to generate RNAi resistant annular furrow mutants with RNAi active in either the intestine (*nhx-2p::rde-1*) or epidermis (*lin-26p::rde-1*). As shown in Figure 7D, *rde-1(ne219)* eliminated or greatly reduced suppression of cytoprotective gene expression by *drl-1* dsRNA in *dpy-10* worms as expected; rescue of *rde-1* in either the epidermis or intestine partially rescued suppression of *gpdh-1*, *hmit-1.1*, *gst-10*, and *nlp-29* by *drl-1* dsRNA and fully rescued suppression of *gst-4*. Therefore, *drl-1* is required in both tissues for full activation of cytoprotective genes by furrow collagen mutation.

Discussion

The *C. elegans* cuticle has emerged as a barrier extracellular matrix sensor for damage that regulates environmental stress responses (Lamitina *et al.* 2006; Pujol *et al.* 2008a; Dodd *et al.* 2018). Annular furrows are a central factor in this signaling mechanism (Dodd *et al.* 2018). Loss of any one of six specific collagens (*dpy-2*, *3*, *7*, *8*, *9*, or *10*) disrupts furrow organization in the adult cuticle and constitutively activates osmolyte accumulation, detoxification, and antimicrobial peptide genes *via* distinct sets of transcription factors (Dodd *et al.* 2018). Other signal transduction mechanisms downstream from this putative mechanosensor remain largely unknown.

DRL-1 functions downstream from furrow disruption to regulate cytoprotection

Our screen for suppression of cytoprotective gene expression in a furrow collagen mutant identified several candidate protein kinases with *drl-1* dsRNA having the most consistent effects on all three stress responses (Figure 1). A model integrating our DRL-1

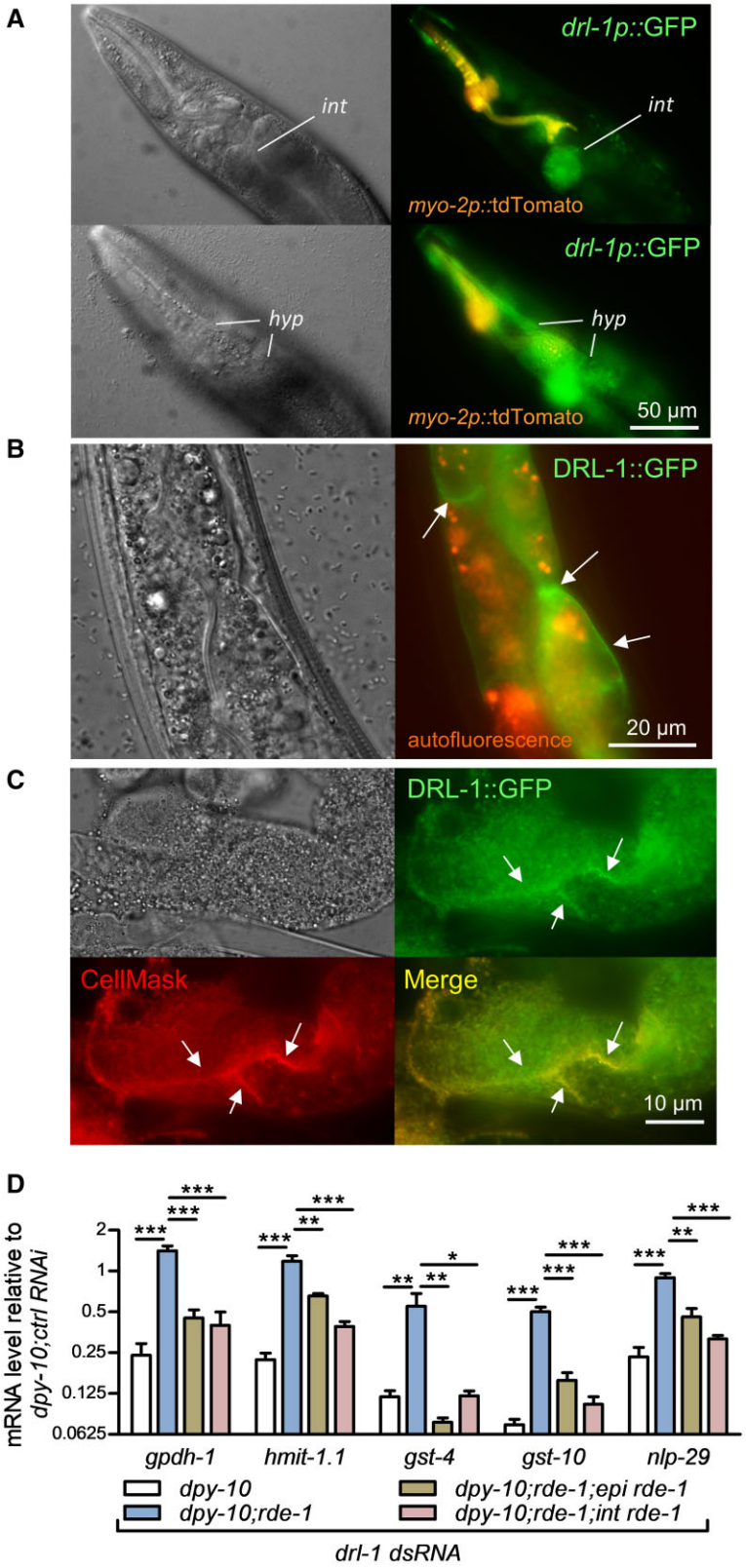

Figure 7 DRL-1 is at or near cellular membranes and functions in the epidermis and intestine. (A–C) Representative DIC and fluorescent micrographs of worms carrying an extrachromosomal array that includes 2.6 kb upstream and intron 1 (A) or the entire *drl-1* gene minus intron 1 (B,C) fused to GFP. (A,B) Fluorescence is a composite of GFP and RFP channels; yellow/orange is *myo-2p*::tdTomato in (A) and orange is auto-fluorescence in (B). White arrows indicate GFP signal at or near cell boundaries. (C) Representative DIC and fluorescent micrographs of excised intestines of worms expressing DRL-1::GFP fusion protein. Excised intestines were treated with CellMask dye (red), fixed, and imaged. White arrows indicate putative cell boundaries. A Pearson's correlation coefficient of 0.69 was calculated in the intestine. (D) mRNA levels in *dpy-10(e128)* mutants; some strains carry *rde-1(n219)* and *rde-1* rescue constructs. $N = 5–6$ populations of worms from 2 trials, $^{***}P < 0.001$, $^{**}P < 0.01$, and $^{*}P < 0.05$.

results with previous understanding of DRL-1 function is shown in Figure 8. Our genetic interaction and collagen::GFP results indicate that DRL-1 functions downstream from the furrow-associated damage sensor and OSM proteins to permit full activation of cytoprotective genes (Figures 2–4). Loss of *drl-1* also suppressed the same stress responses induced by moderate hypertonicity, albeit by a reduced degree for osmolyte accumulation and antimicrobial genes (Figure 5); it is likely that other parallel signaling mechanisms can compensate under this condition (Lee and Strange 2012; Choe 2013). Alternatively, *drl-1* had no role in activation of detoxification genes by oxidative stress or in activation of *nlp-29* by a molting defect consistent with specificity (Figures S2B and S4).

DRL-1 loss in *C. elegans* has been linked to an NHR-49-dependent dietary restriction-like state, resulting in increased fat catabolism and lifespan extension (Chamoli *et al.* 2014). Our results with dietary restriction inducing mutant *eat-2* and *nhr-49* indicate that DRL-1 controls stress response gene expression in furrow collagen mutants independently of this metabolic shift and the signals controlling it (Figure 6). Therefore, DRL-1 has separate functions in at least two distinct physiological contexts, extracellular damage sensor signal transduction and regulation of a dietary restriction-like state (Figure 8).

DRL-1 was previously shown to have protein kinase activity *in vitro*, suggesting that DRL-1 may transduce signals *via* phosphorylation (Chamoli *et al.* 2014). The kinase domain of DRL-1 has 40.3% amino acid similarity to human MEKK3 (Figure S6). MEKK3 has been reported to regulate MAPK signaling cascades including p38, JNK, and ERK (Chang and Karin 2001; Johnson and Lapadat 2002; Padda *et al.* 2006; Kim *et al.* 2007; Pastuhov *et al.* 2015; Kong *et al.* 2019). Within the context of cytoprotection, MEKK3 has been implicated in regulating osmotic stress responses *via* p38 MAPK in mammalian cells (Uhlik *et al.* 2003; Padda *et al.* 2006; Craig *et al.* 2008). *Caenorhabditis elegans* p38 MAPK regulates detoxification and antimicrobial responses (Kim *et al.* 2002; Inoue *et al.* 2005; Blackwell *et al.* 2015; Wu *et al.* 2016) making it a candidate target of DRL-1. However, our data with p38 MAPKK *sek-1* indicates that p38 mediates cytoprotective responses in furrow mutants largely independent of DRL-1 (Figure S5). Future studies are required to determine if DRL-1 functions through other potential downstream signaling pathways including the ones identified in our screen (Figure 1B).

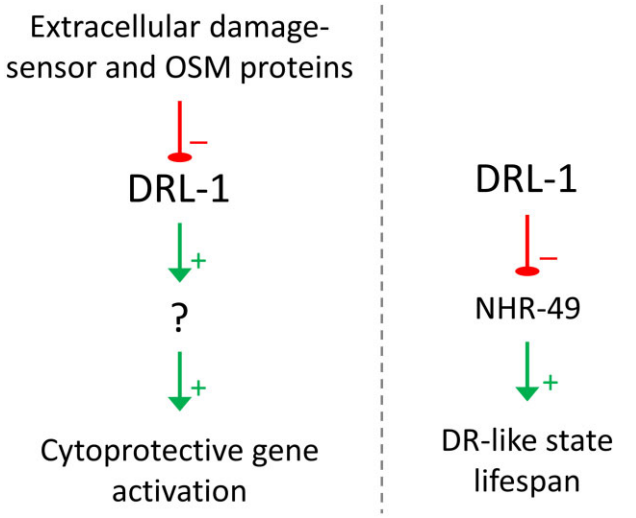

Figure 8 Working model for DRL-1 function. Prior work demonstrated that DRL-1 functions to suppress a dietary-restriction like state mediated by NHR-49 (Chamoli *et al.* 2014). Our results indicate that DRL-1 also functions downstream from a cuticle-based extracellular damage sensor and OSM proteins to permit full activation of cytoprotective genes.

DRL-1 contains atypical C-terminal transmembrane domains

In addition to an N-terminal protein kinase domain, DRL-1 possesses an atypical hydrophobic C-terminus. Transmembrane prediction programs, such as TMpred (Hofmann 1993) and TMHMM2 (Möller *et al.* 2001), predict three transmembrane domains in the C-terminus (Figure S6). Protein kinases with transmembrane domains at the C-terminus are rare; most eukaryotic membrane kinases are receptor tyrosine protein kinases that have N-terminal extracellular receptor and transmembrane domains and a C-terminal intracellular kinase domain (Lemmon and Schlessinger 2010). There is one other protein in *C. elegans* with the same atypical structure, FLR-4 (FLuoride Resistant). FLR-4 also contains an N-terminal serine/threonine protein kinase domain and a C-terminal hydrophobic domain that has 56% amino acid similarity to DRL-1 (Figure S6). FLR-4 regulates longevity (Verma *et al.* 2018) and defecation rhythm in the intestine together with ion channel FLR-1 (Take-uchi *et al.* 2005). Surprisingly, expression of FLR-4 variants that were kinase-dead or missing the entire kinase domain were able to rescue defecation rhythm indicating the importance of the C-terminal hydrophobic domain (Kobayashi *et al.* 2011). Unfortunately, a null *drl-1* mutant is not available and is likely to be inviable. However, future studies with a balanced null or rescue of *drl-1* RNAi with *C. briggsae drl-1* variants could be used to test the relative roles of DRL-1 kinase and transmembrane regions.

DRL-1 may function at the cell membrane

Given potential expression at the plasma membrane (Figure 7), DRL-1 may be able to receive signals from the extracellular environment and transduce intracellular signals as a protein kinase. This model is similar to the CDC42–STE50–STE11–Pbs2 complex in *Saccharomyces cerevisiae* and the Rac–OSM–MEKK3–MKK3 complex in mammalian cells (Uhlik *et al.* 2003; Tatebayashi *et al.* 2006; Zhou *et al.* 2011). In both of these systems, cell volume changes are detected by osmo/mechano-sensors at the cell membrane (SHO1 in yeast, condensed actin ruffles in mammals) (Uhlik *et al.* 2003; Tatebayashi *et al.* 2006; Zhou *et al.* 2011). Intracellular Hog1 and p38 MAPK phosphorylation cascades are then activated in yeast and mammalian cells, respectively leading to activation of cytoprotective genes (Uhlik *et al.* 2003; Tatebayashi *et al.* 2006; Zhou *et al.* 2011).

DRL-1 may also function as part of an osmosensor complex at the membrane. MEKK3 is recruited near the membrane of mammalian cells by scaffold protein OSM during hyperosmolarity (Uhlik *et al.* 2003). DRL-1 is likely constitutively targeted to membranes by its transmembrane domains (Figure 7) where it could also interact with structural filaments. Actin bundles in epidermal cells are associated with furrows during the molting cycle and could also play a role during cuticle damage (Costa *et al.* 1997; McMahon *et al.* 2003). Future screens for interacting proteins could identify other proteins functioning as part of a putative membrane sensor.

Data availability

Strains are available upon request. Raw numeric data are at figshare (https://doi.org/10.6084/m9.figshare.16435221).

Supplementary material is available at *GENETICS* online.

Acknowledgments

Some *C. elegans* strains were obtained from the *Caenorhabditis* Genetics Center (University of Minnesota, Minneapolis, MN, USA) which is supported by the National Institutes of Health Office of Research Infrastructure Programs (P40 OD010440).

Both authors designed experiments, analyzed data, wrote drafts of the manuscript, and approved the final version of the manuscript. K.W. performed the experiments.

Funding

This study was supported by National Science Foundation grants IOS-1120130 and IOS-1452948 to K.P.C and a William Townsend Porter Fellowship funded by the American Physiological Society to K.W.

Conflicts of interest

The authors declare that there is no conflict of interest.

Literature cited

Arner P. 2005. Human fat cell lipolysis: biochemistry, regulation and clinical role. Best Pract Res Clin Endocrinol Metab. 19:471–482.

Beck FX, Burger-Kentischer A, Müller E. 1998. Cellular response to osmotic stress in the renal medulla. Pflugers Arch. 436:814–827.

Blackwell TK, Steinbaugh MJ, Hourihan JM, Ewald CY, Isik M. 2015. SKN-1/Nrf, stress responses, and aging in *Caenorhabditis elegans*. Free Radic Biol Med. 88:290–301.

Blazie SM, Geissel HC, Wilky H, Joshi R, Newbern J, *et al.* 2017. Alternative polyadenylation directs tissue-specific miRNA targeting in *Caenorhabditis elegans* somatic tissues. Genetics. 206:757–774.

Brenner S. 1974. The genetics of *Caenorhabditis elegans*. Genetics. 77: 71–94.

Burkewitz K, Choe KP, Lee EC, Deonarine A, Strange K. 2012. Characterization of the proteostasis roles of glycerol accumulation, protein degradation and protein synthesis during osmotic stress in *C. elegans*. PLoS One. 7:e34153.

Cannon WB. 1929. Organization for physiological homeostasis. Physiol Rev. 9:399–431.

Chamoli M, Singh A, Malik Y, Mukhopadhyay A. 2014. A novel kinase regulates dietary restriction-mediated longevity in *Caenorhabditis elegans*. Aging Cell. 13:641–655.

Chang L, Karin M. 2001. Mammalian MAP kinase signalling cascades. Nature. 410:37–40.

Chisholm AD, Hsiao TI. 2012. The *Caenorhabditis elegans* epidermis as a model skin. I: development, patterning, and growth. Wiley Interdiscip Rev Dev Biol. 1:861–878.

Chisholm AD, Xu S. 2012. The *Caenorhabditis elegans* epidermis as a model skin. II: differentiation and physiological roles. Wiley Interdiscip Rev Dev Biol. 1:879–902.

Choe KP. 2013. Physiological and molecular mechanisms of salt and water homeostasis in the nematode *Caenorhabditis elegans*. Am J Physiol Regul Integr Comp Physiol. 305:R175–R186.

Choe KP, Przybysz AJ, Strange K. 2009. The WD40 repeat protein WDR-23 functions with the CUL4/DDB1 ubiquitin ligase to regulate nuclear abundance and activity of SKN-1 in *Caenorhabditis elegans*. Mol Cell Biol. 29:2704–2715.

Choe KP, Strange K. 2007a. Evolutionarily conserved WNK and Ste20 kinases are essential for acute volume recovery and survival after hypertonic shrinkage in *Caenorhabditis elegans*. Am J Physiol Cell Physiol. 293:C915–927.

Choe KP, Strange K. 2007b. Molecular and genetic characterization of osmosensing and signal transduction in the nematode *Caenorhabditis elegans*. FEBS J. 274:5782–5789.

Chuang C-F, Bargmann CI. 2005. A Toll-interleukin 1 repeat protein at the synapse specifies asymmetric odorant receptor expression via ASK1 MAPKKK signaling. Genes Dev. 19:270–281.

Costa M, Draper BW, Priess JR. 1997. The role of actin filaments in patterning the *Caenorhabditis elegans* cuticle. Dev Biol. 184: 373–384.

Cox GN, Kusch M, Edgar RS. 1981. Cuticle of *Caenorhabditis elegans*: its isolation and partial characterization. J Cell Biol. 90:7–17.

Craig EA, Stevens MV, Vaillancourt RR, Camenisch TD. 2008. MAP3Ks as central regulators of cell fate during development. Dev Dyn. 237:3102–3114.

Danziger J, Zeidel ML. 2015. Osmotic homeostasis. Clin J Am Soc Nephrol. 10:852–862.

Dodd W, Tang L, Lone JC, Wimberly K, Wu CW, *et al.* 2018. A damage sensor associated with the cuticle coordinates three core environmental stress responses in *Caenorhabditis elegans*. Genetics. 208:1467–1482.

Dresen A, Finkbeiner S, Dottermusch M, Beume JS, Li Y, *et al.* 2015. *Caenorhabditis elegans* OSM-11 signaling regulates SKN-1/Nrf during embryonic development and adult longevity and stress response. Dev Biol. 400:118–131.

Fontana L, Partridge L, Longo VD. 2010. Extending healthy life span–-from yeast to humans. Science. 328:321–326.

Fulda S, Gorman AM, Hori O, Samali A. 2010. Cellular stress responses: cell survival and cell death. Int J Cell Biol. 2010: 214074.

Han S, Schroeder EA, Silva-Garcia CG, Hebestreit K, Mair WB, *et al.* 2017. Mono-unsaturated fatty acids link H3K4me3 modifiers to *C. elegans* lifespan. Nature. 544:185–190.

Hasegawa K, Miwa S, Isomura K, Tsutsumiuchi K, Taniguchi H, *et al.* 2008. Acrylamide-responsive genes in the nematode *Caenorhabditis elegans*. Toxicol Sci. 101:215–225.

Hobert O. 2002. PCR fusion-based approach to create reporter gene constructs for expression analysis in transgenic *C. elegans*. Biotechniques. 32:728–730.

Hofmann K. 1993. TMbase-A database of membrane spanning proteins segments. Biol Chem Hoppe-Seyler. 374:166.

Inoue H, Hisamoto N, An JH, Oliveira RP, Nishida E, *et al.* 2005. The *C. elegans* p38 MAPK pathway regulates nuclear localization of the transcription factor SKN-1 in oxidative stress response. Genes Dev. 19:2278–2283.

Johnson GL, Lapadat R. 2002. Mitogen-activated protein kinase pathways mediated by ERK, JNK, and p38 protein kinases. Science. 298:1911–1912.

José De Rosa M, Veuthey T, Florman J, Grant J, Blanco G, *et al.* 2018. Acute-stress impairs cytoprotective mechanisms through neural inhibition of the insulin pathway. bioRxiv. 294645. doi: 10.1101/294645.

Kage-Nakadai E, Uehara T, Mitani S. 2011. H^+/myo-inositol transporter genes, *hmit-1.1* and *hmit-1.2*, have roles in the osmoprotective response in *Caenorhabditis elegans*. Biochem Biophys Res Commun. 410:471–477.

Kamath RS, Fraser AG, Dong Y, Poulin G, Durbin R, *et al.* 2003. Systematic functional analysis of the *Caenorhabditis elegans* genome using RNAi. Nature. 421:231–237.

Kim DH, Feinbaum R, Alloing G, Emerson FE, Garsin DA, *et al.* 2002. A conserved p38 MAP kinase pathway in *Caenorhabditis elegans* innate immunity. Science. 297:623–626.

Kim K, Duramad O, Qin X-F, Su B. 2007. MEKK3 is essential for lipopolysaccharide-induced interleukin-6 and granulocyte-

macrophage colony-stimulating factor production in macrophages. Immunology. 120:242–250.
Kishimoto S, Uno M, Nishida E. 2018. Molecular mechanisms regulating lifespan and environmental stress responses. Inflamm Regen. 38:22.
Kobayashi Y, Kimura KD, Katsura I. 2011. Ultradian rhythm in the intestine of *Caenorhabditis elegans* is controlled by the C-terminal region of the FLR-1 ion channel and the hydrophobic domain of the FLR-4 protein kinase. Genes Cells. 16:565–575.
Komatsu H, Chao MY, Larkins-Ford J, Corkins ME, Somers GA, *et al.* 2008. OSM-11 facilitates LIN-12 Notch signaling during *Caenorhabditis elegans* vulval development. PLoS Biol. 6:e196.
Kong Y-L, Wang Y-F, Zhu Z-S, Deng Z-W, Chen J, *et al.* 2019. Silencing of the MEKK2/MEKK3 pathway protects against spinal cord injury via the hedgehog pathway and the JNK pathway. Mol Ther Nucleic Acids. 17:578–589.
Lakowski B, Hekimi S. 1998. The genetics of caloric restriction in *Caenorhabditis elegans*. Proc Natl Acad Sci USA. 95:13091–13096.
Lamitina ST, Morrison R, Moeckel GW, Strange K. 2004. Adaptation of the nematode *Caenorhabditis elegans* to extreme osmotic stress. Am J Physiol Cell Physiol. 286:C785–791.
Lamitina ST, Strange K. 2005. Transcriptional targets of DAF-16 insulin signaling pathway protect *C. elegans* from extreme hypertonic stress. Am J Physiol Cell Physiol. 288:C467–C474.
Lamitina T, Huang CG, Strange K. 2006. Genome-wide RNAi screening identifies protein damage as a regulator of osmoprotective gene expression. Proc Natl Acad Sci USA. 103:12173–12178.
Lee EC, Strange K. 2012. GCN-2 dependent inhibition of protein synthesis activates osmosensitive gene transcription via WNK and Ste20 kinase signaling. Am J Physiol Cell Physiol. 303:C1269–C1277.
Lee KZ, Kniazeva M, Han M, Pujol N, Ewbank JJ. 2010. The fatty acid synthase fasn-1 acts upstream of WNK and Ste20/GCK-VI kinases to modulate antimicrobial peptide expression in *C. elegans* epidermis. Virulence. 1:113–122.
Lemmon MA, Schlessinger J. 2010. Cell signaling by receptor tyrosine kinases. Cell. 141:1117–1134.
Lewis KN, Mele J, Hayes JD, Buffenstein R. 2010. Nrf2, a guardian of healthspan and gatekeeper of species longevity. Integr Comp Biol. 50:829–843.
Lin Y, Sui LC, Wu RH, Ma RJ, Fu HY, *et al.* 2018. Nrf2 inhibition affects cell cycle progression during early mouse embryo development. J Reprod Dev. 64:49–55.
McMahon L, Muriel JM, Roberts B, Quinn M, Johnstone IL. 2003. Two sets of interacting collagens form functionally distinct substructures within a *Caenorhabditis elegans* extracellular matrix. Mol Biol Cell. 14:1366–1378.
Möller S, Croning MD, Apweiler R. 2001. Evaluation of methods for the prediction of membrane spanning regions. Bioinformatics. 17:646–653.
Oliveira RP, Porter Abate J, Dilks K, Landis J, Ashraf J, *et al.* 2009. Condition-adapted stress and longevity gene regulation by *Caenorhabditis elegans* SKN-1/Nrf. Aging Cell. 8:524–541.
Padda R, Wamsley-Davis A, Gustin MC, Ross R, Yu C, *et al.* 2006. MEKK3-mediated signaling to p38 kinase and TonE in hypertonically stressed kidney cells. Am J Physiol Renal Physiol. 291:F874–F881.
Page AP, Johnstone IL, 2007. The Cuticle. WormBook. doi/10.1895/-wormbook.1.138.1,http://www.wormbook.org.
Pastuhov S, Hisamoto N, Matsumoto K. 2015. MAP kinase cascades regulating axon regeneration in *C. elegans*. Proc Jpn Acad Ser B Phys Biol Sci. 91:63–75.
Pathare PP, Lin A, Bornfeldt KE, Taubert S, Van Gilst MR. 2012. Coordinate regulation of lipid metabolism by novel nuclear receptor partnerships. PLoS Genet. 8:e1002645.
Patterson RA, Juarez MT, Hermann A, Sasik R, Hardiman G, *et al.* 2013. Serine proteolytic pathway activation reveals an expanded ensemble of wound response genes in *Drosophila*. PLoS One. 8: e61773.
Pauli F, Liu Y, Kim YA, Chen PJ, Kim SK. 2006. Chromosomal clustering and GATA transcriptional regulation of intestine-expressed genes in *C. elegans*. Development. 133:287–295.
Przybysz AJ, Choe KP, Roberts LJ, Strange K. 2009. Increased age reduces DAF-16 and SKN-1 signaling and the hormetic response of *Caenorhabditis elegans* to the xenobiotic juglone. Mech Ageing Dev. 130:357–369.
Pujol N, Cypowyj S, Ziegler K, Millet A, Astrain A, *et al.* 2008a. Distinct innate immune responses to infection and wounding in the *C. elegans* epidermis. Curr Biol. 18:481–489.
Pujol N, Zugasti O, Wong D, Couillault C, Kurz CL, *et al.* 2008b. Anti-fungal innate immunity in *C. elegans* is enhanced by evolutionary diversification of antimicrobial peptides. PLoS Pathog. 4: e1000105.
Qadota H, Inoue M, Hikita T, Koppen M, Hardin JD, *et al.* 2007. Establishment of a tissue-specific RNAi system in *C. elegans*. Gene. 400:166–173.
Rohlfing A-K, Miteva Y, Hannenhalli S, Lamitina T. 2010. Genetic and physiological activation of osmosensitive gene expression mimics transcriptional signatures of pathogen infection in *C. elegans*. PLoS One. 5:e9010.
Rohlfing A-K, Miteva Y, Moronetti L, He L, Lamitina T. 2011. The *Caenorhabditis elegans* mucin-like protein OSM-8 negatively regulates osmosensitive physiology via the transmembrane protein PTR-23. PLoS Genet. 7:e1001267.
Sadowska A, Kameda T, Krupkova O, Wuertz-Kozak K. 2018. Osmosensing, osmosignalling and inflammation: how intervertebral disc cells respond to altered osmolarity. Eur Cell Mater. 36: 231–250.
Sandoval LE, Jiang H, Wang D. 2019. The dietary restriction-like gene *drl-1*, which encodes a putative serine/threonine kinase, is essential for orsay virus infection in *Caenorhabditis elegans*. J Virol. 93: e0140001418.
Shore DE, Carr CE, Ruvkun G. 2012. Induction of cytoprotective pathways is central to the extension of lifespan conferred by multiple longevity pathways. PLoS Genet. 8:e1002792.
Singh K, Chao MY, Somers GA, Komatsu H, Corkins ME, *et al.* 2011. *C. elegans* Notch signaling regulates adult chemosensory response and larval molting quiescence. Curr Biol. 21:825–834.
Solomon A, Bandhakavi S, Jabbar S, Shah R, Beitel GJ, *et al.* 2004. *Caenorhabditis elegans* OSR-1 regulates behavioral and physiological responses to hyperosmotic environments. Genetics. 167: 161–170.
Sørensen OE, Thapa DR, Roupé KM, Valore EV, Sjöbring U, *et al.* 2006. Injury-induced innate immune response in human skin mediated by transactivation of the epidermal growth factor receptor. J Clin Invest. 116:1878–1885.
Spencer WC, Zeller G, Watson JD, Henz SR, Watkins KL, *et al.* 2011. A spatial and temporal map of *C. elegans* gene expression. Genome Res. 21:325–341.
Take-Uchi M, Kobayashi Y, Kimura KD, Ishihara T, Katsura I. 2005. FLR-4, a novel serine/threonine protein kinase, regulates defecation rhythm in *Caenorhabditis elegans*. Mol Biol Cell. 16:1355–1365.
Tanaka-Hino M, Sagasti A, Hisamoto N, Kawasaki M, Nakano S, *et al.* 2002. SEK-1 MAPKK mediates Ca^{2+} signaling to determine neuronal asymmetric development in *Caenorhabditis elegans*. EMBO Rep. 3:56–62.
Tang L, Choe KP. 2015. Characterization of *skn-1/wdr-23* phenotypes in *Caenorhabditis elegans*; pleitrophy, aging, glutathione, and

interactions with other longevity pathways. Mech Ageing Dev. 149:88–98.

Tatebayashi K, Yamamoto K, Tanaka K, Tomida T, Maruoka T, *et al.* 2006. Adaptor functions of Cdc42, Ste50, and Sho1 in the yeast osmoregulatory HOG MAPK pathway. EMBO J. 25:3033–3044.

Tebay LE, Robertson H, Durant ST, Vitale SR, Penning TM, *et al.* 2015. Mechanisms of activation of the transcription factor Nrf2 by redox stressors, nutrient cues, and energy status and the pathways through which it attenuates degenerative disease. Free Radic Biol Med. 88:108–146.

Thacker C, Peters K, Srayko M, Rose AM. 1995. The *bli-4* locus of *Caenorhabditis elegans* encodes structurally distinct kex2/subtilisin-like endoproteases essential for early development and adult morphology. Genes Dev. 9:956–971.

Thein MC, McCormack G, Winter AD, Johnstone IL, Shoemaker CB, *et al.* 2003. *Caenorhabditis elegans* exoskeleton collagen COL-19: an adult-specific marker for collagen modification and assembly, and the analysis of organismal morphology. Dev Dyn. 226: 523–539.

Uhlik MT, Abell AN, Johnson NL, Sun W, Cuevas BD, *et al.* 2003. Rac–MEKK3–MKK3 scaffolding for p38 MAPK activation during hyperosmotic shock. Nat Cell Biol. 5:1104–1110.

van der Kammen R, Song J-Y, de Rink I, Janssen H, Madonna S, *et al.* 2017. Knockout of the Arp2/3 complex in epidermis causes a psoriasis-like disease hallmarked by hyperactivation of transcription factor Nrf2. Development. 144:4588–4603.

Van Gilst MR, Hadjivassiliou H, Jolly A, Yamamoto KR. 2005. Nuclear hormone receptor NHR-49 controls fat consumption and fatty acid composition in *C. elegans*. PLoS Biol. 3:e53.

Verma S, Jagtap U, Goyala A, Mukhopadhyay A. 2018. A novel gene-diet pair modulates *C. elegans* aging. PLoS Genet. 14: e1007608.

Wang Y, Alam T, Hill-Harfe K, Lopez AJ, Leung CK, *et al.* 2013. Phylogenetic, expression, and functional analyses of anoctamin homologs in *Caenorhabditis elegans*. Am J Physiol Regul Integr Comp Physiol. 305:R1376–R1389.

Wheeler JM, Thomas JH. 2006. Identification of a novel gene family involved in osmotic stress response in *Caenorhabditis elegans*. Genetics. 174:1327–1336.

Wu CW, Deonarine A, Przybysz A, Strange K, Choe KP. 2016. The Skp1 homologs SKR-1/2 are required for the *Caenorhabditis elegans* SKN-1 antioxidant/detoxification response independently of p38 MAPK. PLoS Genet. 12:e1006361.

Wu CW, Wang Y, Choe KP. 2017. F-Box protein XREP-4 is a new regulator of the oxidative stress response in *Caenorhabditis elegans*. Genetics. 206:859–871.

Zhang Y, Li W, Li L, Li Y, Fu R, *et al.* 2015. Structural damage in the *C. elegans* epidermis causes release of STA-2 and induction of an innate immune response. Immunity. 42:309–320.

Zhou X, Izumi Y, Burg MB, Ferraris JD. 2011. Rac1/osmosensing scaffold for MEKK3 contributes via phospholipase C-gamma1 to activation of the osmoprotective transcription factor NFAT5. Proc Natl Acad Sci USA. 108:12155–12160.

Ziegler K, Kurz CL, Cypowyj S, Couillault C, Pophillat M, *et al.* 2009. Antifungal innate immunity in *C. elegans* links G protein signaling and a conserved p38 MAPK Cascade. Cell Host Microbe. 5: 341–352.

Zugasti O, Thakur N, Belougne J, Squiban B, Kurz CL, *et al.* 2016. A quantitative genome-wide RNAi screen in *C. elegans* for antifungal innate immunity genes. BMC Biol. 14:35.

Communicating editor: B. Goldstein